Suppression of "Edge MHD Instability of LHD" by External RMP

Shu ITO[1)], Kiyomasa WATANABE[1,2)], Yuki TAKEMURA[2,3)], Satoru SAKAKIBARA[2,3)] and Sadao MASAMUNE[4)]

[1)]*Nagoya University, Graduate School of Engineering, Chikusa, Nagoya 464-8603, Japan*
[2)]*National Institute for Fusion Science, National Institutes of Natural Sciences, Toki, Gifu 509-5292, Japan*
[3)]*SOKENDAI (The Graduate University for Advanced Studies), Toki, Gifu 509-5292, Japan*
[4)]*Chubu University, Graduate School of Engineering, Kasugai, Aichi 487-8501, Japan*

(Received 18 October 2023 / Accepted 20 November 2023)

We experimentally investigate the effect of external resonant magnetic perturbation (RMP) on"Edge MHD instability", which is observed in a discharge with relatively low magnetic Reynolds number and middle beta in the Large Helical Device (LHD) and leads to minor collapse (rapid degradation of volum-averaged beta value by 10%). When the external RMP is small, the instability is continuously observed in a discharge, and the fluctuation amplitude decreases a little with the increment of the RMP. When the RMP is large enough, the appearance of the instability becomes intermittent, and the fluctuation amplitude rapidly decreases with the increment of the RMP. Moreover, the confinement performance degraded by the instability also recovers when the intermittent instability appears.

Keywords: LHD, MHD instability, RMP, magnetic confinement, helical plasma

DOI: 10.1585/pfr.19.1402001

1. Introduction

In order to develop economical nuclear fusion reactors with magnetically confined torus plasma, we need to stably confine more than 5% of volume-averaged beta plasma in a reactor core. One of the main tasks in achieving the development is suppression or avoidance of MHD instabilities. In the Large Helical Device (LHD) [1], 5% of volume-averaged beta discharges without collapse phenomena have already been achieved [2]. In the above 5% of volume-averaged beta discharges, fluctuations due to low-order resistive interchange instabilities in the peripheral region are frequently observed, and they prevent further increase of the beta value [3, 4]. On the contrary, the following collapse phenomena, which are observed as rapid degradation of the beta value by more than 10%, due to the MHD instabilities are observed in the certain operational conditions in the LHD. (1) The MHD instability in core region. (2) "Core density collapse (CDC)" due to ballooning instability. (3) "Locked-mode-like instability". (4) "Edge MHD instability".

Avoiding the operational range, where the instabilities with collapse are expected to appear, might be effective to maintain the discharges without collapse. However, it is important to find the way to suppress the instabilities with collapse because there is a possibility that we cannot avoid the operational range to access the higher beta region. As shown in a previous research result on the instability suppression in the LHD, applying resonant magnetic perturbation (RMP) by external coils is effective to suppress the magnetic activity due to low-n resistive interchange instability, which is often observed in the LHD high beta discharges equivalent to nuclear fusion reactors [5]. Except for this, there is little research about suppression of resistive interchange instability by the external RMP. On the other hand, in tokamaks, it is also well-known that imposing external RMP is effective for stabilization of MHD instabilities such as tearing and/or locked mode [6], resistive wall mode (RWM) [7] and edge localized mode (ELM) [8].

In this paper, we apply the external RMP to "$m/n = 1/1$ edge MHD instability" and investigate its effect on the instability. Here, 'm' and 'n' indicate poloidal and toroidal mode numbers, respectively. It is known that "$m/n = 1/1$ edge MHD instability" appears in the magnetic configurations like $3.65\,\mathrm{m} < R_{ax} < 3.78\,\mathrm{m}$ with relatively low magnetic Reynolds number and middle beta, when the $m/n = 1/1$ resonant surface becomes close to the plasma boundary [9]. Here, "R_{ax}" is a torus major radial location of the magnetic axis. Note that, in the LHD, the magnetic well depth/hill height is sensitive to the magnetic axis torus location. The main characteristics of "$m/n = 1/1$ edge MHD instability" are much different from those of $m/n = 1/1$ resistive interchange instability. As shown in Ref. [9], "$m/n = 1/1$ edge MHD instability" has the following characteristics. (1) After it grows, collapse occurs. (2) After the collapse, the flattening of the radial electron temperature profile around the resonant surface is kept, and the electron temperature inside the resonant surface much degrades compared before the collapse. (3) The frequency of the magnetic field fluctuation is about half of that due

author's e-mail: ito.shu@nifs.ac.jp

to $m/n = 1/1$ resistive interchange instability. (4) It always has a higher harmonic with $m/n = 2/2$. (5) Both fluctuation amplitude of the magnetic field and the electron density is much larger than that due to resistive interchange instability. (6) It has a tearing-parity in the mode structure. Note that resistive interchange instability has an interchange-parity, as shown in Sec. 2.

This paper describes the active control of "$m/n = 1/1$ edge MHD instability" by the external RMP. In Secs. 2 and 3, we mention the experimental set-up, and the typical response of "$m/n = 1/1$ edge MHD instability" to the external RMP compared with that of resistive interchange instability, respectively. Finally, in Sec. 4, we give a summary.

2. Experimental Set-Up

The LHD is a type of the helical system. It is equipped with a pair of helical coils and three pairs of poloidal coils. Its typical major radius, R_{ax}, is 3.5 ~ 4.0 m and the minor radius, a_p, is 0.46 ~ 0.64 m. In the LHD, we can control the rotational transform profile (magnetic shear) and the height of the magnetic hill through changing R_{ax} and the shape of the plasma poloidal cross-section, which are changed through control of the current ratio between poloidal coils [10]. Here, we experimentally investigate how "$m/n = 1/1$ edge MHD instability" responds to the applied external RMP compared to $m/n = 1/1$ resistive interchange instability. In detail, we use the static $m/n = 1/1$ external RMP with different amplitude in every discharge, which means it does not rotate and has constant amplitude and phase during a discharge, while two kinds of the instabilities rotate in poloidal and toroidal directions. In the above experiments, the resonant magnetic surface of $\iota = 1$ is located at $r/a_p \sim 0.9$ in vacuum, where "r" is plasma minor radius. Typically, the surface moves to the peripheral region with increase of the beta value, but it always exists in the magnetic hill region during discharges.

In order to compare the response of "$m/n = 1/1$ edge MHD instability" to the external RMP with that of $m/n = 1/1$ resistive interchange instability, we conduct discharges with the same magnetic configuration, with $R_{ax} = 3.75$ m, $R_{ax}/a_p = 6.3$, and the operational magnetic field strength, $B_t = 0.75$ T, under the different plasma parameter ranges where two kinds of the instabilities occur. Figures 1 and 2 show typical waveforms of the discharges with "$m/n = 1/1$ edge MHD instability" and those with $m/n = 1/1$ resistive interchange instability without imposing the external RMP, respectively. Figures 1 (a) and 2 (a) show the time evolution of the volume-averaged beta value, measured by diamagnetic loop [11], and the total port-through power of tangentially injected Neutral Beam (NB). Figures 1 (b) and 2 (b) show the line-averaged electron density measured by far-infrared (FIR) laser interferometer [12] and the total port-through injection power of the two beam lines of the perpendicular NB, one of which is injected as a probe

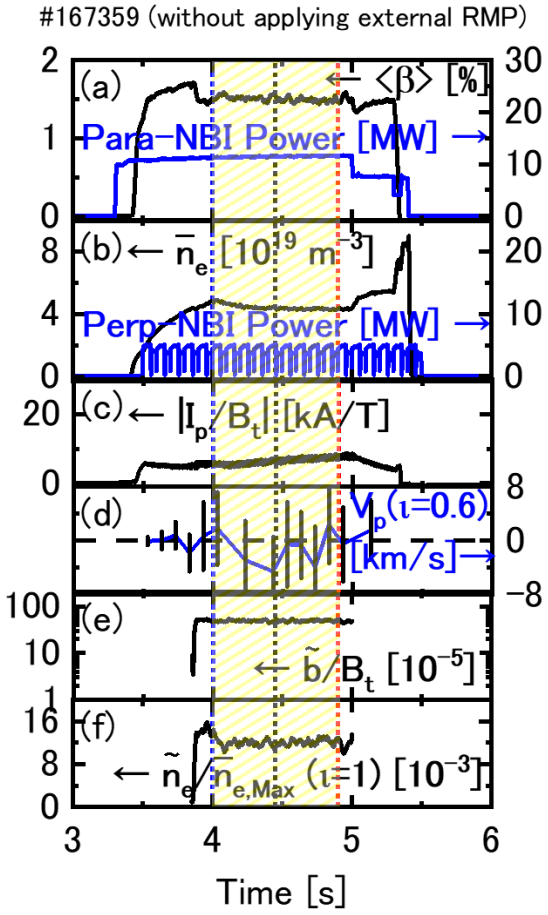

Fig. 1 Typical waveform of a discharge with "$m/n = 1/1$ edge instability". (a) Volume-averaged beta and total tangential NBI port-through power for three beam lines. (b) Line-averaged electron density and total perpendicular NBI port-through power for two beam lines. (c) Plasma current normalized by operational magnetic field strength. (d) Poloidal flow speed around the $\iota = 0.6$ surface. (e) $m/n = 1/1$ magnetic field fluctuation amplitude normalized by operational magnetic field strength. (f) Electron density fluctuation amplitude around the $\iota = 1$ surface, normalized by the maximum time-averaged electron density. Yellow shadow region corresponds to the time window for the analysis. The blue, black and red dotted vertical lines correspond to the beginning, middle and end of the time window for the analysis.

beam to measure the plasma flow speed, and the other is to keep the heating power almost constant during a discharge. The heating powers in Figs. 1 (b) and 2 (b) look intermittent, but the duration time of no-perpendicular NB is much short. Figures 1 (c) and 2 (c) show the plasma current normalized by the operational magnetic field, I_p/B_t. Figures 1 (d) and 2 (d) show the poloidal flow speed measured by charge exchange spectroscopy (CXS) [13]. Note that Fig. 1 (d) corresponds to the data around $\iota = 0.6$ (r/a_p ~ 0.6) because the plasma flow speed around $\iota = 1$ (r/a_p ~ 0.9) is not measured due to high density discharges, and Fig. 2 (d) corresponds to the data around $\iota = 1$. Here, the

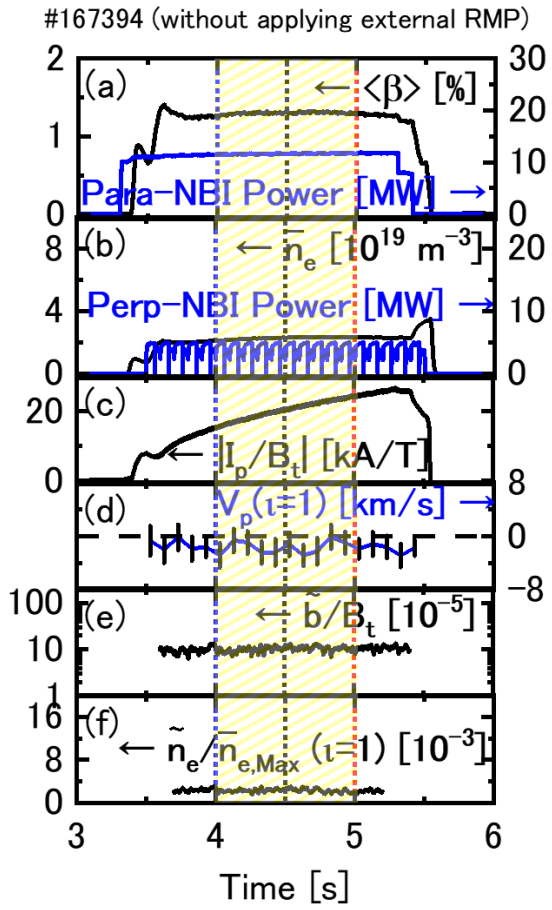

Fig. 2 Typical waveform of a discharge with m/n = 1/1 resistive interchange instability. (a) Volume-averaged beta and total tangential NBI port-through power for three beam lines. (b) Line-averaged electron density and total perpendicular NBI port-through power for two beam lines. (c) Plasma current normalized by operational magnetic field strength. (d) Poloidal flow speed around the ι = 1 surface. (e) m/n = 1/1 magnetic field fluctuation amplitude normalized by operational magnetic field strength. (f) Electron density fluctuation amplitude around the ι = 1 surface, normalized by the maximum time-averaged electron density. Yellow shadow region corresponds to the time window for the analysis. The blue, black and red dotted lines correspond to the beginning, middle and end of the time window for the analysis.

ι = 1 surface is identified from the location of the electron temperature flattening, which is measured by Thomson scattering [14], due to "m/n = 1/1 edge instability" or m/n = 1/1 resistive interchange instability. Figures 1 (e), (f) and 2 (e), (f) show the m/n = 1/1 mode amplitude of the poloidal field fluctuation, measured by magnetic probe [11] outside plasma, and the electron density fluctuation amplitude around the ι = 1 surface which has high coherence with the m/n = 1/1 magnetic field fluctuation, measured by CO2 laser interferometer [15], respectively. Here, note that we consider that the line integrated electron density fluctuation amplitude for measured sight line tangent to the ι = 1 surface is equivalent to the electron density fluctuation amplitude at the local ι = 1 surface. The fluctuation amplitude shown in Figs. 1 (e), (f) and 2 (e), (f) indicates the root mean square (RMS) during 20 ms. We used the data in the yellow shadow region in Figs. 1 and 2 for the analysis because plasma is in an almost steady state. Note that one of NB lines breaks down around t = 5 s in #167359 discharge, as shown in Fig. 1 (a), so we do not use the data during the time range of NB breaking down for the analysis.

In Fig. 1 (a), the rapid degradation of the beta value around t = 3.8 s corresponds to minor collapse. At the same time, both fluctuation amplitude of the magnetic field and the electron density increases rapidly, as shown in Figs. 1 (e) and (f). On the contrary, in Fig. 2, the beta value and the fluctuation amplitude are almost constant during the discharge. In the experiment with "Edge instability", the line-averaged electron density is two times as high as in that with resistive interchange instability, and the volume-averaged beta value is also higher, as shown in Figs. 1 and 2, because "Edge instability" occurs when both electron density and beta value are higher than the certain values, as shown in the previous study [5]. Moreover, both fluctuation amplitude of the magnetic field and the electron density due to "Edge instability" are almost five times as large as that due to resistive interchange instability. It is considered that the observed plasma current mainly consists of Okawa-current because the injection power of NB, which enhances the rotational transform, is stronger than that of NB which reduces it. As the electron density becomes high, Okawa-current decreases with a high energy component due to NB. Then the plasma current in the resistive interchange instability experiment is larger than that in the "Edge instability" experiment. Note that in Figs. 1 (c) and 2 (c), the 20 kA/T of plasma current normalized by the operational magnetic field corresponds to the increment of the rotational transform at the edge by almost 0.04, which means that the plasma current does not affect the MHD equilibrium and stabilities so much.

Figures 3 and 4 show typical radial mode structures observed in a discharge with "m/n = 1/1 edge instability" and in that with m/n = 1/1 resistive interchange instability, respectively. (a), (b) and (c) of Figs. 3 and 4 show the radial profiles of the line integrated density fluctuation amplitude, the phase difference, and the coherence for discharges with "Edge instability" (#167359) and resistive interchange instability (#167394). Note that the reference channel on estimation of the phase difference and the coherence has the maximum fluctuation amplitude, the blue regions in Figs. 3 and 4 correspond to the area around the m/n = 1/1 resonant surface, and the data with red circles to the high coherence. Figure 3 shows a tearing-parity in the radial mode structure. On the contrary, Fig. 4 shows an interchange-parity. Note that in the case of resistive interchange instability, the background of the line integrated fluctuation amplitude is fairly high, and the coherence in

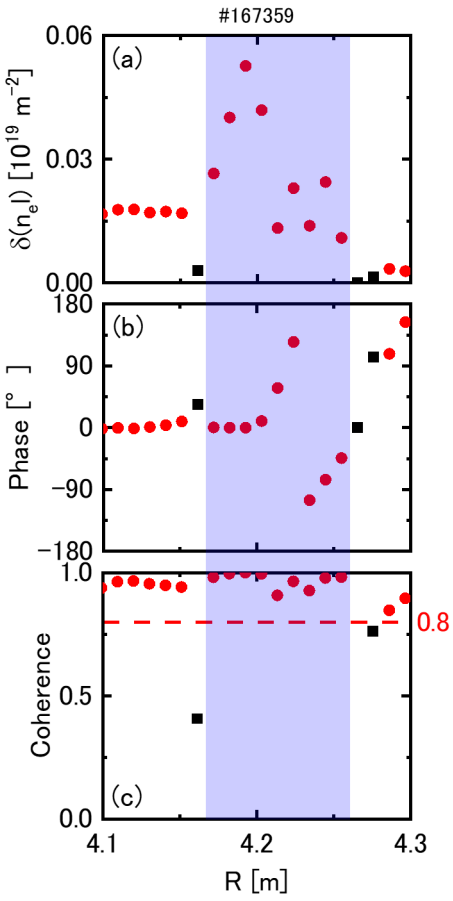

Fig. 3 Typical radial mode structure in a discharge with "m/n = 1/1 edge instability". (a) Line integrated electron density fluctuation amplitude, (b) phase difference and (c) coherence. The reference channel on estimation of the phase difference and the coherence has the maximum fluctuation amplitude. Symbols "●" correspond to the data more than 0.8 in the coherence, and symbols "■" correspond to those less than 0.8. Blue region corresponds to the area around the $\iota = 1$ surface.

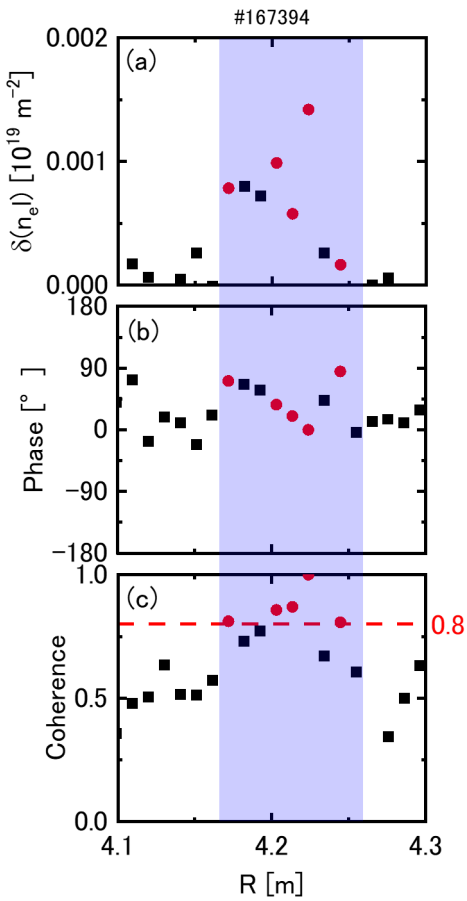

Fig. 4 Typical radial mode structure in a discharge with m/n = 1/1 resistive interchange instability. (a) Line integrated electron density fluctuation amplitude, (b) phase difference and (c) coherence. The reference channel on estimation of the phase difference and the coherence has the maximum fluctuation amplitude. Symbols "●" correspond to the data more than 0.8 in the coherence, and symbols "■" correspond to those less than 0.8. Blue region corresponds to the area around the $\iota = 1$ surface.

radial channels around the resonant surface is not so large.

Figures 5 and 6 show the following three parameters when the amplitude of the external RMP changes for each discharge: (a) the volume-averaged beta value, (b) the line-averaged electron density and (c) the absolute value of the plasma current normalized by the operational magnetic field. Here, note that the amplitude of the external RMP is expressed by the maximum value of the external RMP coils normalized by the operational magnetic field strength, I_{RMP}/B_t. Figures 5 and 6 correspond to the operational parameters of the discharges with "Edge instability" and those with resistive interchange instability, respectively. It is considered that the growth rate of the pressure driven MHD instabilities is strongly affected by the pressure gradient, magnetic shear, and magnetic hill height around the resonant surface. Little difference in the above three parameters in Figs. 5 and 6 correspond to scant divergence in the magnetic shear and magnetic hill height in the discharges with the various levels of the external RMP. Here, we plot the data of three phase in order to show little change in each parameter during the period in which instabilities appear. Note that the external RMP penetrates into the resonant surface beyond the level of the external RMP ($I_{RMP}/B_t > 2.4$ kA/T in Figs. 5 and 6); then the magnetic configurations would be much different from those with the shielding of the external RMP ($I_{RMP}/B_t < 2.3$ kA/T in Figs. 5 and 6). Note that $I_{RMP}/B_t = 1.1$ kA/T is expected through calculation to induce a magnetic island with the width of 20% of the plasma minor radius in the vacuum.

We specially focus on the change of the pressure gradient around the resonant surface, in addition to the fluctuation amplitude of the magnetic field and the electron density as an index how each instability is unstable. Note that the pressure profile is evaluated under the assumption that $n_i = n_e$, $T_i = T_e$ and $Z_{eff} = 1$, and the electron density radial profile which is evaluated from the line integrated one

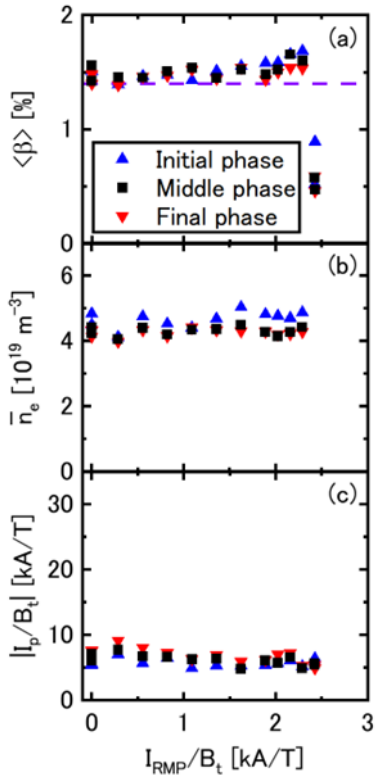

Fig. 5 Response of typical plasma parameters to external RMP in the experiment with "Edge instability". (a) Volume-averaged beta, (b) line-averaged electron density and (c) plasma current normalized by operational magnetic field strength, as a function of the external RMP coil current normalized by operational magnetic field strength. Symbols "▲", "■" and "▼" correspond to the beginning, middle and end phase of the time window for the analysis shown in Fig. 1, respectively. Purple horizontal dashed line in (a) indicates the volume-averaged beta in the discharge without applying external RMP.

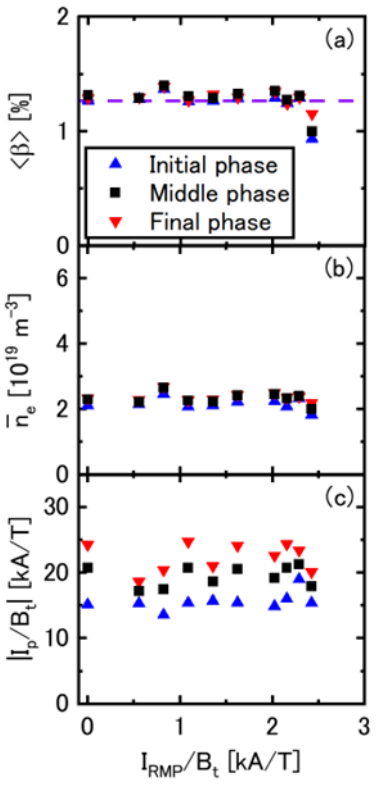

Fig. 6 Response of typical plasma parameters to external RMP in the experiment with resistive interchange instability. (a) Volume-averaged beta, (b) line-averaged electron density and (c) plasma current normalized by operational magnetic field strength, as a function of the external RMP coil current normalized by operational magnetic field strength. Symbols "▲", "■" and "▼" correspond to the beginning, middle and end phase of the time window for the analysis shown in Fig. 2, respectively. Purple horizontal dashed line in (a) indicates the volume-averaged beta in the discharge without applying external RMP.

by Abel inversion [5]. Here, n_i, n_e, T_i, T_e and Z_{eff} are the ion and electron density and temperature, and the effective electric charge, respectively.

3. Response of "$M/N = 1/1$ Edge MHD Instability" to External RMP

In this section, we show experimental results of the response of "Edge instability" to the external RMP, compared with that of resistive interchange instability under the same operational conditions without the line-averaged electron density and the volume-averaged beta value.

Figures 7 and 8 show the response of "$m/n = 1/1$ edge instability" and $m/n = 1/1$ resistive interchange instability to the external RMP, respectively. Table 1 shows the operational conditions of the above experiments. We analyse 14 discharges with 1.5% volume-averaged beta value for "Edge instability", and 10 discharges with 1.3% volume-averaged beta value for resistive interchange instability. Figures 7 (a) and 8 (a) show the $m/n = 1/1$ magnetic field fluctuation amplitude, as a function of the normalized external RMP coil current, I_{RMP}/B_t. Figures 7 (b) and 8 (b) show the electron density fluctuation amplitude at the $\iota = 1$ surface, which is the resonant surface of the $m/n = 1/1$ mode. Note that, in Figs. 7 (a) and (b), there are two data

Table 1 Experimental condition of discharges of Figs. 7 and 8.

Shot	14	10
B_t	0.75 [T]	0.75 [T]
R_{ax}	3.75 [m]	3.75 [m]
B_γ	1.254	1.254
B_q	100	100
$\bar{n}_e$	4.4 [$\times 10^{19} m^{-3}$]	2.2 [$\times 10^{19} m^{-3}$]
<β>	1.5 [%]	1.3 [%]
Minor collapse	With	Without

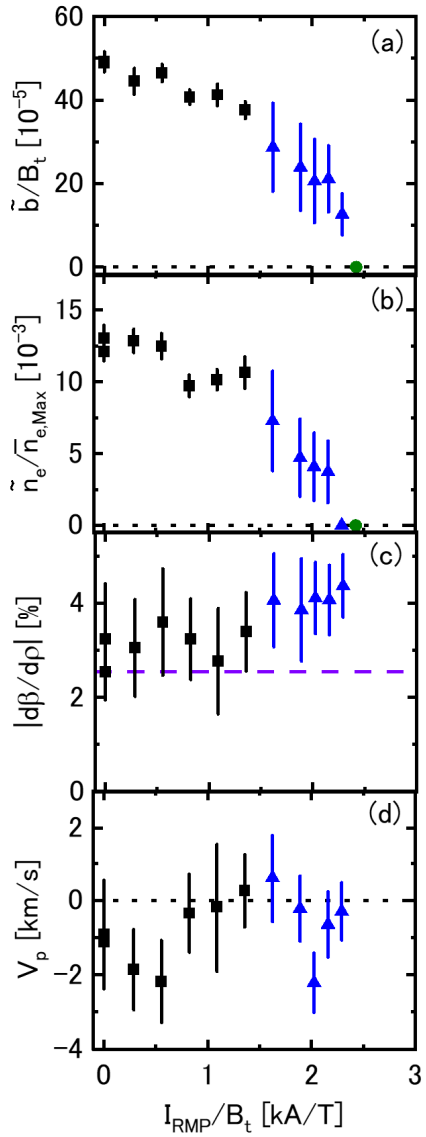

Fig. 7 Response of "$m/n = 1/1$ edge instability" to external RMP. (a) Magnetic field fluctuation amplitude with $m/n = 1/1$, normalized by operational magnetic field strength, (b) electron density fluctuation amplitude around the $\iota = 1$ surface, normalized by the maximum time-averaged electron density, (c) beta gradient around the $\iota = 1$ surface and (d) poloidal flow speed around the $\iota = 0.6$ surface, as a function of the external RMP coil current normalized by operational magnetic field strength. Symbols "■" indicate the discharges with continuous appearance of "Edge instability", and symbols "▲" indicate those with intermittent appearance. Symbols "●" indicate the discharges with external RMP penetration to the $\iota = 1$ surface. Purple horizontal dashed line in (c) indicates the beta gradient in the discharge without applying external RMP.

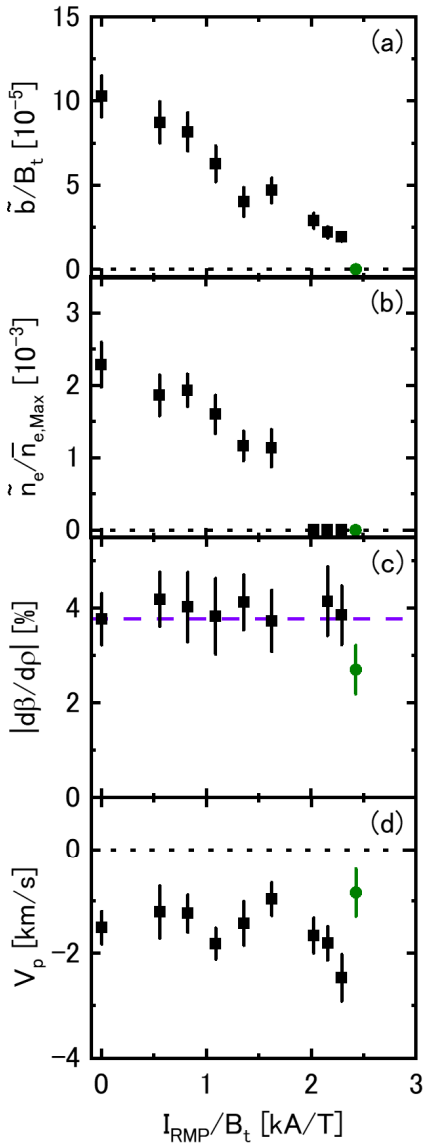

Fig. 8 Response of $m/n = 1/1$ resistive interchange instability to external RMP. (a) Magnetic field fluctuation amplitude with $m/n = 1/1$, normalized by operational magnetic field strength, (b) electron density fluctuation amplitude around the $\iota = 1$ surface, normalized by the maximum time-averaged electron density, (c) beta gradient and (d) poloidal flow speed around the $\iota = 1$ surface, as a function of the external RMP coil current normalized by operational magnetic field strength. Symbols "■" and "●" indicate the discharges without and with external RMP penetration to the $\iota = 1$ surface, respectively. Purple horizontal dashed line in (c) indicates the beta gradient in the discharge without applying external RMP.

with almost the same value around $I_{RMP}/B_t \sim 2.4$ kA/T. Figures 7 (c) and 8 (c) show the absolute value of the beta gradient at the $\iota = 1$ surface. Note that the beta gradient corresponds to the averaged value between the torus-inside and outside data. Figures 7 (d) and 8 (d) show the poloidal flow speed. Note that Fig. 7 (d) corresponds to the data around $\iota = 0.6$, and Fig. 8 (d) to the data around $\iota = 1$. All data in Figs. 7 and 8 indicate the time-averaged value of the data during the time window for the analysis, as shown by the yellow shadow region in Figs. 1 and 2. In Figs. 7 and 8 (a) to (d), error bars indicate the range of square root of the variance.

The absolute value of the beta gradient indicated by "■" or "▲" in the region of $I_{RMP}/B_t < 2.3$ kA/T of Figs. 7 and 8 is kept almost equal to or greater than that without applying the external RMP, whose level is indicated by the purple dashed line. On the contrary, in $I_{RMP}/B_t > 2.4$ kA/T, the static large flattening region in the electron temperature profile is observed, and the amplitude of the beta gradient discontinuously decreases. Here it is considered that the external RMP penetration to the $m/n = 1/1$ resonant surface induces the decrease of the beta gradient through the formation of a magnetic island. Note that in the discharges with "Edge instability", the pressure gradient in $I_{RMP}/B_t > 2.4$ kA/T in Fig. 7 cannot be evaluated because the radial electron density profile is not obtained by Abel inversion due to the formation of the large magnetic island. Moreover, as shown in Fig. 7 (c), the beta gradient in $I_{RMP}/B_t > 1.6$ kA/T (shown by "▲") is larger than that in $I_{RMP}/B_t < 1.4$ kA/T (shown by "■"). However, in Figs. 7 (a), (b), 8 (a) and (b), both fluctuation amplitude of the magnetic field and the electron density decreases as the external RMP coil current increases, which indicates that the degree of "edge instability" decreases as well as resistive interchange instability. Note that in the range of $I_{RMP}/B_t = 2.3$ kA/T in Fig. 7 and 2.0 kA/T $< I_{RMP}/B_t <$ 2.3 kA/T in Fig. 8, though the finite coherent magnetic field fluctuation exists, the coherent electron density fluctuation does not exist, because the later tends to have lower coherence than the former. In the range of $I_{RMP}/B_t > 2.4$ kA/T, the magnetic field fluctuation amplitude is zero, as shown by "●" in Figs. 7 and 8. There, both instabilities become stabilized, because the external RMP penetration to the $m/n = 1/1$ resonant surface induces the decrease of the beta gradient through the formation of a magnetic island.

Now we focus on the difference of the two instabilities' response to the external RMP. In resistive interchange instability, as shown in Figs. 8 (a) and (b), the decreasing rate of the fluctuation amplitude of the magnetic field and the electron density is monotonical when the external RMP coil current increases. On the contrary, in "Edge instability", as shown in Figs. 7 (a) and (b), the decreasing rate in the region of $I_{RMP}/B_t > 1.6$ kA/T (shown by "▲"), is larger than that in $I_{RMP}/B_t < 1.4$ kA/T (shown by "■"), which means that "Edge instability" is suppressed more greatly in high external RMP cases. Moreover, both time-averaged beta gradient and volume-averaged beta value in $I_{RMP}/B_t > 1.6$ kA/T increase more clearly than those in $I_{RMP}/B_t < 1.4$ kA/T, as shown in Figs. 7 (c) and 5 (a). The above result indicates that applying relatively strong external RMP leads to clear improvement of the confinement performance, through great suppression of "Edge instability".

Next, we consider the reason why the decreasing rate of the time-averaged fluctuation amplitude on the external RMP amplitude for "Edge instability" changes discontinuously. Figures 9 to 11 show the time evolution of (a) the volume-averaged beta value, (b) the $m/n = 1/1$ magnetic field fluctuation amplitude and (c) the electron density fluctuation amplitude around the resonant surface, respectively. Figures 9, 10 and 11 correspond to the cases of $I_{RMP}/B_t = 1.4$ kA/T, 1.6 kA/T and 2.2 kA/T, respectively. In Fig. 9, which indicates a typical case of $I_{RMP}/B_t < 1.4$ kA/T (shown by "■" in Fig. 7), the magnetic field and electron density fluctuation amplitude increase rapidly around $t = 3.9$ s, when minor collapse happens, and the clearly large fluctuation amplitude and small beta value are kept continuously during the time window for the analysis, indicated by the yellow shadow region in Fig. 9. On the contrary, in Figs. 10 and 11, which indicate typical cases of $I_{RMP}/B_t > 1.6$ kA/T (shown by "▲" in Fig. 7), the fluctuation amplitude sometimes becomes small and then the beta value becomes large after occurrence of "Edge instability" during the time window for the analysis. Here, in Fig. 10, the time window for the analysis is shorter than in Figs. 9 and 11 because of NB breaking down. Note that the error in Figs. 7 (a) and (b) is large because it is estimated from the square root of the variance of the time-averaged value and "Edge instability" occurs intermittently and repeatedly in the region of $I_{RMP}/B_t > 1.6$ kA/T (shown by "▲").

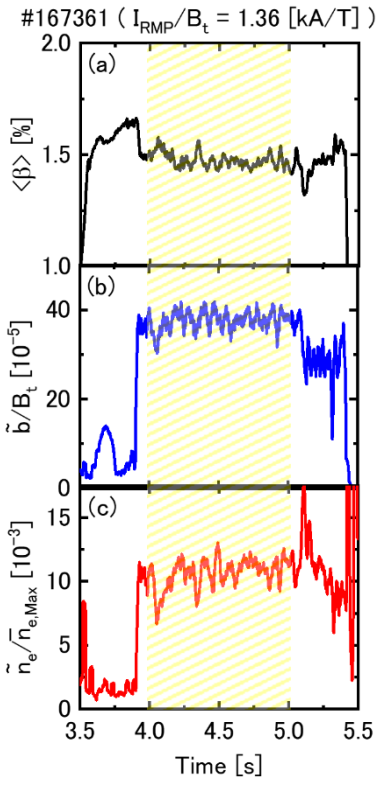

Fig. 9 In $I_{RMP}/B_t = 1.4$ kA/T, time evolution of (a) volume-averaged beta, (b) magnetic field fluctuation amplitude with $m/n = 1/1$, normalized by operational magnetic field strength and (c) electron density fluctuation amplitude around the $\iota = 1$ surface, normalized by the maximum time-averaged electron density, respectively. Yellow shadow region corresponds to the time window for the analysis.

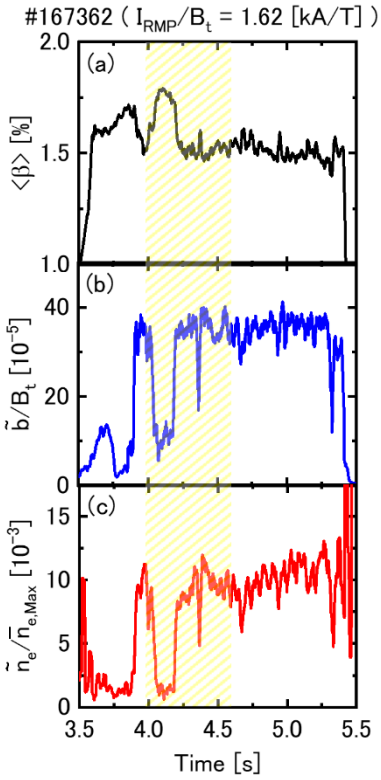

Fig. 10 In I_{RMP}/B_t = 1.6 kA/T, time evolution of (a) volume-averaged beta, (b) magnetic field fluctuation amplitude with m/n = 1/1, normalized by operational magnetic field strength and (c) electron density fluctuation amplitude around the ι = 1 surface, normalized by the maximum time-averaged electron density, respectively. Yellow shadow region corresponds to the time window for the analysis.

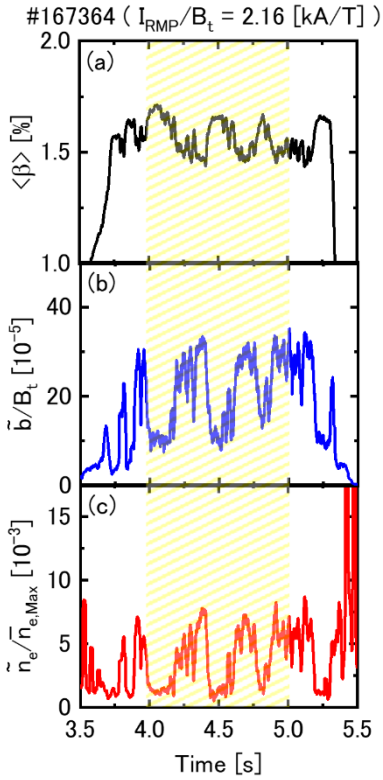

Fig. 11 In I_{RMP}/B_t = 2.2 kA/T, time evolution of (a) volume-averaged beta, (b) magnetic field fluctuation amplitude with m/n = 1/1, normalized by operational magnetic field strength and (c) electron density fluctuation amplitude around the ι = 1 surface, normalized by the maximum time-averaged electron density, respectively. Yellow shadow region corresponds to the time window for the analysis.

Then, we consider that both decreasing rate of the time-averaged fluctuation amplitude of the magnetic field and electron density in $I_{RMP}/B_t > 1.6$ kA/T becomes larger than in $I_{RMP}/B_t < 1.4$ kA/T because "Edge instability" occurs intermittently. Moreover, from Figs. 10 and 11, it is found that in I_{RMP}/B_t = 2.2 kA/T, the duration time, when both fluctuation amplitude is clearly large, is shorter than in I_{RMP}/B_t = 1.6 kA/T. On the contrary, the duration time, when the volume-averaged beta value is relatively high, is opposite to the above. Figure 12 shows the ratio of the duration time, when the fluctuation amplitude of the magnetic field and electron density due to "Edge instability" are clearly large, to the time window for the analysis, as a function of the external RMP coil current. In the region of 1.6 kA/T $< I_{RMP}/B_t <$ 2.3 kA/T indicated by purple in Fig. 12, the above ratio decreases monotonically as the external RMP amplitude increases.

On the effect of the poloidal flow speed on the stabilization of the MHD instabilities, previous research has shown its small effect on that of resistive interchange instability [5]. In the case of "Edge instability", as shown in Fig. 7 (d), the absolute value of the poloidal flow speed

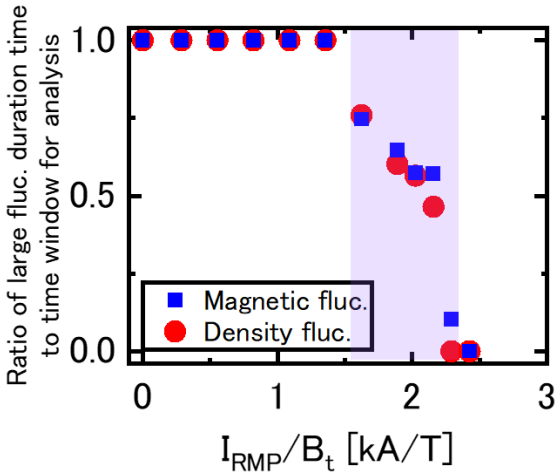

Fig. 12 Ratio of duration time, when the fluctuation amplitude is clearly a large value, to the time window for the analysis, as a function of the external RMP coil current normalized by operational magnetic field strength. Purple region corresponds to the range, where "m/n = 1/1 edge instability" is observed intermittently. Symbols "■" and "●" correspond to the magnetic field fluctuation amplitude with m/n = 1/1, normalized by operational magnetic field strength, and the electron density fluctuation amplitude around the ι = 1 surface, normalized by the maximum time-averaged electron density, respectively.

around the $\iota = 0.6$ surface decreases once as the external RMP amplitude increases. Here, it should be noted that the poloidal flow speed shown in Fig. 7 (d) is for $\iota \sim 0.6$, because the flow speed around $\iota = 1$ is not measured due to high density discharges. Then, the effect of the poloidal flow speed on the stabilization of "Edge instability" is not clear. It is one of the future subjects.

4. Summary and Conclusion

We experimentally investigate the effect of the external RMP on "Edge MHD instability" in the LHD, which has a tearing-parity in the mode structure and induces the large degradation of plasma confinement property. The characteristics are quite different from resistive interchange instability which is often observed in the LHD discharges. We impose the static $m/n = 1/1$ external RMP, which does not rotate and has constant amplitude and phase during a discharge, on plasmas with "$m/n = 1/1$ edge instability" and change the RMP amplitude in every discharge. We compare the RMP effect on "Edge MHD instability" with that on resistive interchange instability under the same magnetic configuration and heating condition but different line-averaged electron density and volume-averaged beta value.

As the common response of "Edge instability" with resistive interchange instability to the external RMP, we obtain the following results. As the external RMP increases, both magnetic field and electron density fluctuation amplitude, which indicates the degree of the instability, decreases. Moreover, the beta gradient around the resonant surface, which is a driving source of a pressure driven instability, is kept almost equal to or larger than that in the discharges, without applying the external RMP. As a different behaviour on the response of "Edge instability" to the external RMP from resistive interchange instability, we obtain the following results. In "Edge instability", the relatively strong external RMP makes the decreasing rate of the fluctuation amplitude of the magnetic field and electron density become larger. On the contrary, both fluctuation amplitude decreases monotonically in the resistive interchange instability. The reason for the change in the decreasing rate of the fluctuation amplitude is that "Edge instability" occurs intermittently. That means that both large fluctuations of the magnetic field and electron density appear intermittently, and the ratio of the duration time of appearance of the large fluctuation to the time window for the analysis decreases as the external RMP amplitude increases. Moreover, when the external RMP is relatively strong, the confinement performance improves more clearly than in discharges where the large fluctuation appears continuously.

From the above results, applying the external RMP can suppress "Edge instability", which has a tearing-parity in the mode structure, as well as resistive interchange instability, which has an interchange-parity. However, the response of the two instabilities is different. The stabilization mechanism of "Edge instability" by the external RMP has not been understood yet, nor has that of resistive interchange instability. So, to resolve the mechanism is our main subject in the near future.

Acknowledgments

The author (S. Ito) would like to thank the "Nagoya University Interdisciplinary Frontier Fellowship" supported by JST and Nagoya University. The authors also thank to the LHD experiment group for their excellent support. In addition, this work was supported by NIFS under contract KIPP008, by JSPS KAKENHI (No.20K03910), and by a grant from the Future Energy Research Association.

[1] M. Osakabe, H. Takahashi, H. Yamada, K. Tanaka, T. Kobayashi, K. Ida, S. Ohdachi, J. Varela, K. Ogawa, M. Kobayashi *et al.*, Nucl. Fusion **62**, 042019 (2022).
[2] S. Sakakibara, K.Y. Watanabe, Y. Suzuki, Y. Narushima, S. Ohdachi, N. Nakajima, F. Watanabe, L. Garcia, A. Weller, K. Toi *et al.*, Plasma Phys. Control. Fusion **50**, 124014 (2008).
[3] S. Ohdachi, Y. Suzuki, H. Tsuchiya, K.Y. Watanabe, S. Sakakibara, Y. Narushima, X.D. Du, T.F. Ming, M. Furukawa, K. Toi *et al.*, Nucl. Fusion **55**, 093006 (2015).
[4] S. Sakakibara, K.Y. Watanabe, H. Funaba, Y. Suzuki, S. Ohdachi, K. Ida, K. Tanaka, T. Tokuzawa, T. Morisaki, M. Osakabe *et al.*, Nucl. Fusion **57**, 066007 (2017).
[5] S. Ito, K.Y. Watanabe, Y. Takemura, S. Sakakibara and S. Masamune, Nucl. Fusion **63**, 066016 (2023).
[6] M. Okabayashi, P. Zanca, E.J. Strait, A.M. Garofalo, J.M. Hanson, Y. In, R.J. La Haye, L. Marrelli, P. Martin, R. Paccagnella *et al.*, Nucl. Fusion **57**, 016035 (2017).
[7] Y.Q. Liu and A. Bondeson, Phys. Rev. Lett. **84**, 907 (2000).
[8] T.E. Evans, R.A. Moyer, P.R. Thomas, J.G. Watkins, T.H. Osborne, J.A. Boedo, E.J. Doyle, M.E. Fenstermacher, K.H. Finken, R.J. Groebner *et al.*, Phys. Rev. Lett. **92**, 235003 (2004).
[9] Y. Takemura, K.Y. Watanabe, S. Sakakibara, S. Ohdachi, Y. Narushima, K. Tanaka and T. Tokuzawa, Phys. Plasmas **29**, 092505 (2022).
[10] K.Y. Watanabe, S. Masamune, Y. Takemura, H. Funaba, S. Sakakibara, F. Watanabe, K. Tanaka, S. Ohdachi, K. Toi, Y. Narushima and LHD Experimaent Group, Phys. Plasmas **18**, 056119 (2011).
[11] S. Sakakibara, H. Yamada and LHD Experiment Group, Fusion Sci. Technol. **58**, 471 (2010).
[12] T. Akiyama, K. Kawahata, K. Tanaka, T. Tokuzawa, Y. Ito, S. Okajima, K. Nakayama, C.A. Michael, L.N. Vyacheslavov, A. Sanin *et al.*, Fusion Sci. Technol. **58**, 352 (2010).
[13] K. Ida, S. Kado and Y. Liang, Rev. Sci. Instrum. **71**, 2360 (2000).
[14] I. Yamada, K. Narihara, H. Funaba, T. Minami, H. Hayashi, T. Kohmoto and LHD Experiment Group, Fusion Sci. Technol. **58**, 345 (2010).
[15] K. Tanaka, C. Michael, L. Vyacheslavov, A. Sanin, K. Kawahata, S. Okajima, T. Akiyama, T. Tokuzawa and Y. Ito, Plasma Fusion Res. **2**, S1033 (2007).